Performance Enhancement of Intermediate Temperature SOFC Cathode by Nano-Composite Coating

[1]Saim Saher, [2]Kamran Alam, [3]Affaq Qamar, [4]Abid Ullah, [5]Javed Iqbal

[1]Advanced Materials Laboratory (AML), Renewable Energy Engineering (REE), U.S.-Pakistan Center for Advanced Studies in Energy (USPCAS-E), UET Peshawar, Pakistan

[1,2,4]Materials for Energy Storage and Conversion (MESC), U.S.-Pakistan Center for Advanced Studies in Energy (USPCAS-E), UET Peshawar, Pakistan

[3]Electrical Energy System Engineering (EESE), U.S.-Pakistan Center for Advanced Studies in Energy (USPCAS-E), UET Peshawar, Pakistan

[5]Department of Electrical Engineering, Sarhad University of Science and Information Technology, Peshawar, Pakistan

Corresponding author: Dr. Saim Saher
E-mail address: s.saher@uetpeshawar.edu.pk

Abstract

The $La_{0.6}Sr_{0.4}Co_{0.2}Fe_{0.8}O_{3-\delta}$ (LSCF) is categorized as a mixed ionic-electronic conducting oxide has found significant attention as cathode material in solid oxide fuel cells (SOFCs) operating at intermediate temperatures, $500\text{-}850^oC$. The performance of LSCF electrode is limited by the oxygen ion transport process at the surface, which is the rate determining step of oxygen reduction reaction. To enhance the oxygen surface exchange process of LSCF electrode, a nano-composite electrolyte is introduced at the surface, which substantially improves the electrochemical performance. The electrical conductivity relaxation technique (ECR) has been used to study the oxygen surface exchange kinetics of bare LSCF and coated with a mixture of $Ce_{0.8}Sm_{0.2}O_{2-\delta}$ (SDC) and $ZrO_2.Y_2O_3$ (Yttria-stabilized zirconia - YSZ) nano-powders in three different weight ratios, SDC:YSZ = 0.5:1, 1:1, 1:0.5. The chemical oxygen surface exchange coefficient k_{chem} of surface modified specimens were derived with a one-parameter fitting process. The results show that the oxygen surface exchange kinetics of LSCF is affected by the SDC-YSZ coating and the average kchem values of SDC-YSZ coated LSCF increases by a factor 2 to 8 from 650 to 850 ^oC, respectively. It has been concluded that the high ionic conductive oxide coating improves the oxygen surface exchange kinetics of underlying LSCF mixed conducting oxide and consequently enhances the performance of electrochemical device such as solid oxide fuel cell.

Key words: SOFC, ECR, Nano-composite, Coating

I. Introduction

$La_{0.6}Sr_{0.4}Co_{0.2}Fe_{0.8}O_{3-\delta}$ (LSCF) is mixed conducting perovskite type oxide, which exhibit high ionic and electronic conductivity over a wide temperature range. It has good electrocatalytic activity at temperature lower than $800^{o}C$ [III] [IV] [VI] [X] [XI] [XVI]. Moreover the thermal expansion coefficient of LSCF is well matched with electrolyte materials such as zirconia-based and ceria-based electrolytes. Therefore LSCF is considered as a suitable material to be used as SOFC cathode. Increasing the oxygen reduction reaction (ORR) sites also known as triple phase boundary (TPB) enhances the cell performance of LSCF-based SOFC cathode[II] [V] [VI] [VIII] [IX] [XV][XVIII] [XIX]. There are difference experimental approaches available to enlarge the active surface area for the oxygen exchange kinetics. Precious metals such as Pd, Pt, Ag have been blended with LSCF to increase the performance[XII] [XVII] [XX]. Coating the electrolyte material such as GDC, SDC and LMO on the cathode surface is one of the recent approaches that promote the surface exchange kinetics of LSCF substrate[I] [XIII] [XIV]. Nonetheless, more investigation is needed to understand and explore the surface exchange kinetics of coated phase.

In this study, novel coating approach is adopted to enhance the surface exchange kinetics of LSCF is investigate after decorating the exposed surfaces of substrate with a mixture of $Ce_{0.8}Sm_{0.2}O_{2-\delta}$ (SDC) and$ZrO_2.Y_2O_3$ (Yttria-stabilized zirconia -YSZ) nanoparticles. The results reveal that the deposition of SDC-YSZ has obvious enhancement in the surface exchange kinetics of LSCF composite cathode and proposed material has a potential to be used in SOFC applications.

II. ExperimentalSynthesis of LSCF

The stoichiometric amount of highly pure (99.9 %) lanthanum (III) nitrate hexahydrate, iron (III) nitrate nonahydrate, strontium (II) nitrate and cobalt (II) nitrate hexahydrate were purchased from Sigma Aldrich and used without any further treatment. All the precursors were dissolved in deionized water by EDTA/citrate complexation route. To evaporate the excessive solvent, the solution was continuously stirred and heated at $150^{o}C$ to form a thick gel type texture and then any further heating results in thermal decomposition of the complex to form LSCF perovskite phase. Fig. 1, shows the X-ray powder diffraction pattern of LSCF and confirms the purity of ceramic oxide.
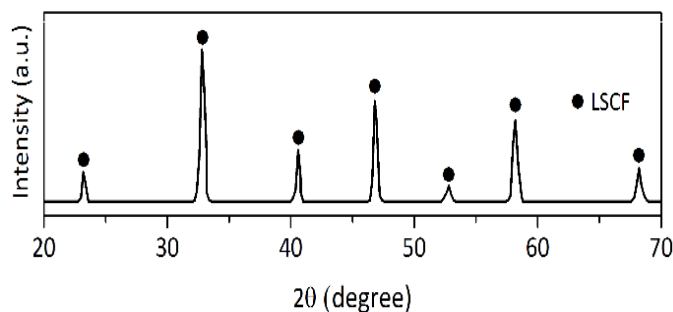

Fig. 1 X-ray diffraction patterns of LSCF powder

III.   Sample Preparation

The obtained fluffy LSCF powder is ball milled for 48 hours in the presence of ethanol. The mixture was dried at room temperature and subsequently calcined at 1000°C to attain a fine powder. Then the power was sieved through 200 μm stainless steel mesh to remove any agglomerated particles. The fine power mend to pellet shape by the application of 15 kPa uniaxial and 300 MPaisostatic pressing. The green compacts were sintered in air at 1200°C for 10 hours using heating and cooling rates of 5°C.min^{-1}. The relative density of sintered pellets were measured by Archimedes method and found in the range of 96% to 98%. The dense ceramics were sized to rectangular thin sheets of 18 mm × 9 mm × 0.6 mm and the largest surfaces were mirror-polished using standard diamond paste. Prior to further use the sheets were ultrasonically cleaned for 10 min in the presence of acetone.

IV.   Nano-particulate Coating

Phase purity of SDC and YSZ nanoparticle were confirmed by X-ray powder diffraction. Prior to the SDC coating over the LSCF rectangular sheets a 5:100 ratio mixture of polyvinyl-butyral (PVB):ethanol was sprayed to form a thin layer of a binding agent. Subsequently, the LSCF sample was inserted in the indigenously developed coating equipment, which produces a dust of SDC-YSZ by a cyclonic action. Time and depth of insertion of LSCF bars inside the coating chamber governs the deposition of coating mixture on the exposed surfaces. Coated samples using innovative coating process was further calcined in stepwise manner in oven at 300 ^{o}C for 3 hours, 700 ^{o}C for 1 hour and 850 ^{o}C for 1 hour for firm binding of SDC-YSZ particles over the LSCF surface. The heating rate was kept at 5 ^{o}C.min^{-1}. Later the coated specimen was sonicated in ethanol to remove the loosely attached SDC-YSZ particles from the sample surface.

V.   Electrical Conductivity Relaxation (ECR) Measurement

A four-probe dc technique was used to measure ECR. The partial pressure of oxygen was maintained between 0.80 and 0.20 atm by appropriate mixing of nitrogen and oxygen gases. The pressure of oxygen was monitored by an oxygen analyzer (Toray zirconia oxygen analyzer). The as-prepared samples were annealed at 850°C for 2 h in oxygen environment to cure the gold painted electrodes before acquiring the ECR measurements. The experiments were run from 650°C to 850°C with 50°C incremental change and oxidation and reduction cycles were repeated for three times at each temperature. The conductivity transient was recorded by instantaneous step change of pO2 between 0.2 to 0.8 atm. The recorded data was normalized and fit to Eq. 1-3 to extract chemical diffusion coefficient (D_{chem}) and the surface exchange coefficient (k_{chem}). The detailed description of the ECR technique and model used for data fitting can be found elsewhere [29].

$$\bar{\sigma}(t)=\frac{\sigma(t)-\sigma_0}{\sigma_\infty-\sigma_0}=1-\prod_{i=x,y}\sum_{m=1}^{\infty}\frac{2L_i^2}{\beta_{m,i}^2(\beta_{m,i}^2+L_i^2+L_i)}\cdot\frac{\tau_{m,i}}{\tau_{m,i}-\tau_f}\cdot\left(\exp(-\frac{t}{\tau_{m,i}})-\frac{\tau_f}{\tau_{m,i}}\exp(-\frac{t}{\tau_f})\right) \tag{1}$$

$$\tau_{m,i}=\frac{b_i^2}{D_{chem}\beta_{m,i}^2} \tag{2}$$

$$L_i=\frac{b_i}{L_c}=\beta_{m,i}\tan\beta_{m,i} \tag{3}$$

X-ray diffraction (XRD) was used to investigate the phase compositions of the prepared cathodes. The microstructures of the cathodes were analyzed using scanning electron microscope (SEM).

VI. Results and Discussion

Deposition behavior of SDC-YSZ nanoparticles on LSCF

Fig. 2, shows the surface morphology of the bare and coated LSCF samples. These SEM images illustrate the dispersion of SDC-YSZ nanoparticles on LSCF substrate. Due to the increase in loading content more SDC-YSZ particles were observed on the LSCF surface, as shown in Fig. 2b, 2c and 2d,. Also, Fig. 2c shows that almost all the LSCF surface is covered by SDC-YSZ particles when 1:1 composition was used.

Upon decreasing SDC ratio in coating mixture, the particles agglomerate and fine dispersion shifts towards the formation of large clusters. With the increase or decrease of SDC-YSZ coating mixture ratios the loading content also varies. Loading content of SDC-YSZ ratios 1:1, 1: 0.5 and 0.5:1are 1.8 mg.cm^{-2} (Fig. 2c), 1.1 mg.cm^{-2} (Fig. 2b), and 0.95 mg.cm^{-2} (Fig. 2d), respectively. Also, for the SDC-YSZ ratios 1:1, 1: 0.5 and 0.5:1, the average coated particle sizes are 0.1, 0.13 and 4.4 μm^2, respectively. The resultant covered surface of LSCF by coated phase varies as SDC-YSZ loading content increases. Ultimately, this effects the active sites of oxidation reduction reactions (ORR) and larger clusters of SDC-YSZ emerged on the LSCF substrate reduces the active sites for oxygen adsorption sites available on the LSCF surface, as shown in Fig. 1d.
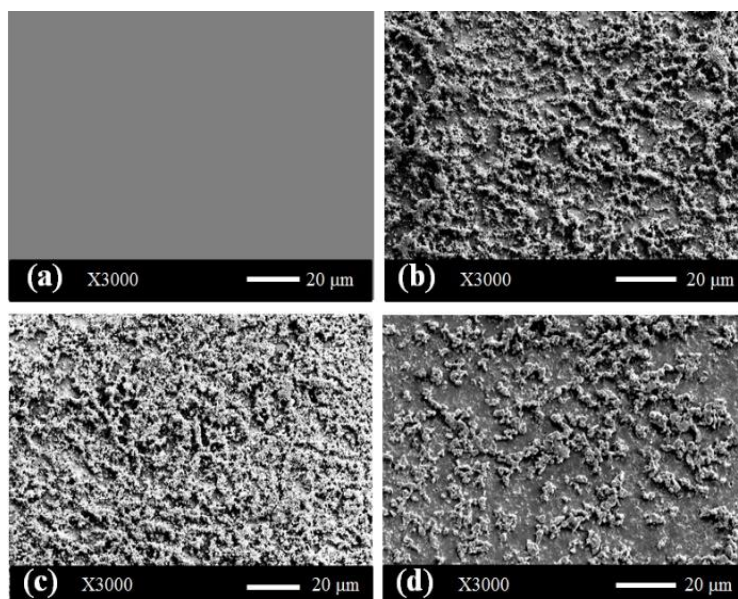
Fig. 2 SEM micrographs of (a) bare LSCF samples, coated LSCF with different SDC-YSZ ratio (b) 1:0.5, (c) 1.1 and (d) 0.5:1.

VII.   Effect of SDC contents on electrochemical performance

Fig. 3, shows the normalized ECR measurements of bare LSCF and SDC-YSZ coated samples at 850 ^{o}C temperature for oxidation run. The partial pressure of oxygen was maintained from 0.2 to 0.8. The time-dependent conductivity increases with the increase in the SDC-YSZ mixture. The results reveals that there is substantial improvement in the oxygen transport kinetics due to SDC-YSZ coating over the LSCF samples. Moreover, the bulk diffusion coefficient, D_{chem}, and surface exchange coefficient, k_{chem}, were calculated by fitting time-dependent conductivity in non-equilibrium solution to Fick's diffusion equation.

Fig. 4, represents the D_{chem} versus temperaturegraph for bare and coated LSCF samples. All the samples have similar values of D_{chem} in the temperature range 650°C to 850°C. This suggests that the surface parameters did not affect the bulk LSCF. Thus surface exchange coefficient is the only contributive factor to enhance the electrochemical performance. The k_{chem}versus temperature graph is obtained with one-parameter fitting by keeping D_{chem} constant shown in Fig. 5. The results show that value of k_{chem} varies with the change in SDC-YSZ loading. The maximum enhancement in k_{chem} is observed for the SDC:YSZ ratio 1:1 at temperature 850 ^{o}C, which is 9.71 x 10^{-5} m.s^{-1}. The value of k_{chem} for bare LSCF sample (1.9 x 10^{-5} m.s^{-1}) is 7 factors less than the SDC:YSZ ratio 1:1 coated sample at the same temperature.
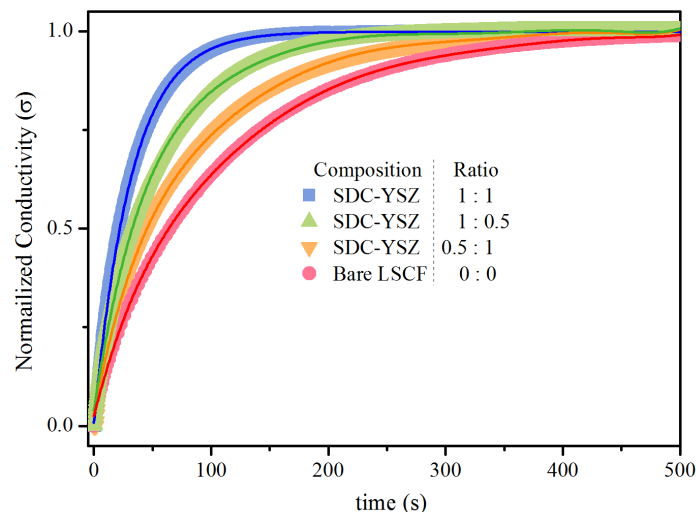
Fig.3 Normalized conductivity curve of bare LSCF, and LSCF/SDC composite during oxidation run only at temperature 850°C (pO$_2$ maintained between 0.8 and 0.2 atm).
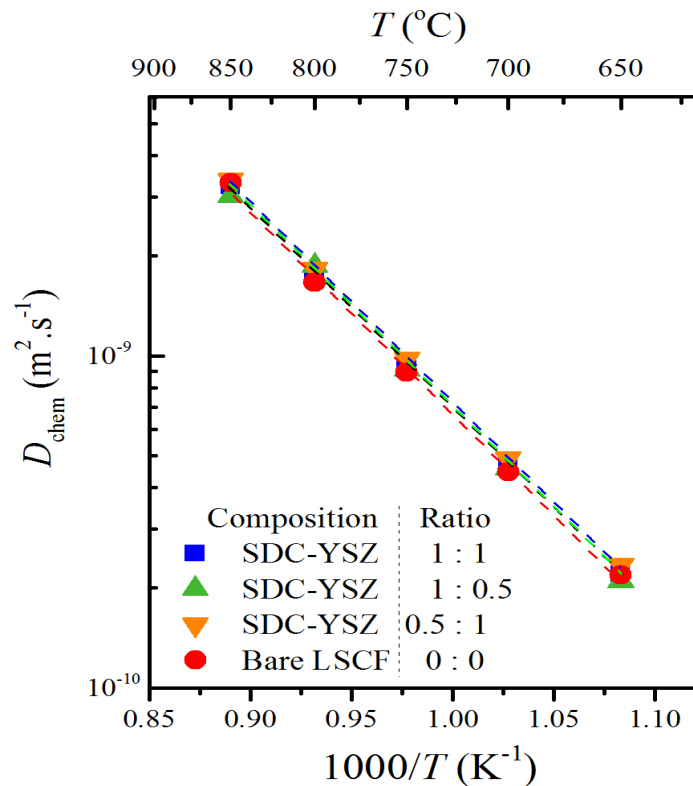

Fig. 4 Arrhenius plot of D_{chem} for bare and coated LSCF samples for oxidation runs only. Extracted data from conductivity transients shows similar values of D_{chem}vs T.
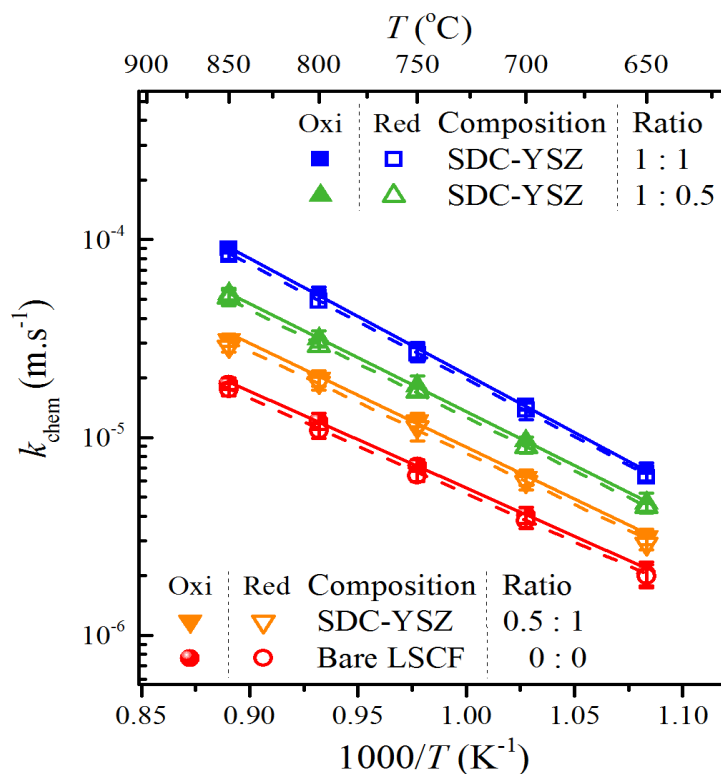
Fig. 5 Arrhenius plot of k_{chem} for bare and coated LSCF samples. Data extracted from conductivity transients recorded after oxidation step changes between 0.8 and 0.2 atm.

The effect of SDC-YSZ contents on the electrochemical performance can be related to the morphology of the SDC-YSZ particles observed over the LSCF substrate (Fig. 2). Since LSCF is a mixed ionic and electronic conducting oxides therefore the ORR occurs at two regions i.e. triple phase boundary (LSCF/SDC-YSZ/oxygen) and double phase boundary (LSCF/oxygen). Since SDC-YSZ mixture has better ionic conductivity therefore, number of active sites was increased when SDC-YSZ mixing ratio was 1:1 with the loading content of 1.8 mg.cm^{-2}. However, further variation in the mixing ratio of SDC-YSZ on LSCF surface either forms larger clusters or non-uniform coverage of SDC-YSZ particles. This hinders the formation of active sites at the TPB and DPB. Thus the selective coating ratio of SDC-YSZ nanoparticles such as 1:1 on LSCF surface significantly improves the surface exchange kinetics. This further improves the adsorption capabilities of oxygen from atmosphere, ionic and electronic conductivities at the electrode surface leading to enhance the electrochemical performance. Thus LSCF with selective coating of SDC-YSZ presents a candidate cathode material for SOFC due to higher oxygen exchange kinetics.

VIII. Conclusions

Adjusting the coating ratio of SDC-YSZ nanopowders improves the surface exchange kinetics of LSCF. The microstructural analysis revealed that expanding the triple phase boundary and double phase boundary of the composite cathode can accelerate the rate of oxygen reduction reactions. This study reveals the importance of SDC-YSZ coating mixture over the LSCF and supports the argument that the SDC-YSZ composite material is a suitable candidate for cathode of IT-SOFC and oxygen separation membrane due to its high oxygen exchange kinetics.

IX. Acknowledgement

Refernces

I.   A.Samreen, S. Saher, S. Ali, H. Shahzad, A. Qamar, Effect of hetero-structured nano-particulate coating on the oxygen surface exchange properties of La0.6Sr0.4Co0.2Fe0.8O3-δ, *Int. Journal of Hydrogen Energy, HE-25296*, 2019 (in press)

II.   Cheng, F., & Chen, J. (2012). Metal–air batteries: from oxygen reduction electrochemistry to cathode catalysts. *Chemical Society Reviews*, *41*(6), 2172-2192.

III.   Fekete, M., Hocking, R. K., Chang, S. L., Italiano, C., Patti, A. F., Arena, F., &Spiccia, L. (2013). Highly active screen-printed electrocatalysts for water oxidation based on β-manganese oxide. *Energy & Environmental Science*, *6*(7), 2222-2232.

IV.   Gorlin, Y., & Jaramillo, T. F. (2010). A bifunctional nonprecious metal catalyst for oxygen reduction and water oxidation. *Journal of the American Chemical Society*, *132*(39), 13612-13614.

V.   Haoran, Y., Lifang, D., Tao, L., & Yong, C. (2014). Hydrothermal synthesis of nanostructured manganese oxide as cathodic catalyst in a microbial fuel cell fed with leachate. *The Scientific World Journal*, *2014*.

VI.   He, G., Qiao, M., Li, W., Lu, Y., Zhao, T., Zou, R., &Parkin, I. P. (2017). S, N- Co- Doped Graphene- Nickel Cobalt Sulfide Aerogel: Improved Energy Storage and Electrocatalytic Performance. *Advanced Science*, *4*(1), 1600214.

VII.   Iyer, A., Del-Pilar, J., King'ondu, C. K., Kissel, E., Garces, H. F., Huang, H., &Suib, S. L. (2012). Water oxidation catalysis using amorphous manganese oxides, octahedral molecular sieves (OMS-2), and octahedral layered (OL-1) manganese oxide structures. *The Journal of Physical Chemistry C*, *116*(10), 6474-6483.

VIII.   Kjaergaard, C. H., Rossmeisl, J., &Nørskov, J. K. (2010). Enzymatic versus inorganic oxygen reduction catalysts: Comparison of the energy levels in a free-energy scheme. *Inorganic chemistry*, *49*(8), 3567-3572.

IX.   Kundu, S., Nagaiah, T. C., Xia, W., Wang, Y., Dommele, S. V., Bitter, J. H., &Muhler, M. (2009). Electrocatalytic activity and stability of nitrogen-containing carbon nanotubes in the oxygen reduction reaction. *The Journal of Physical Chemistry C*, *113*(32), 14302-14310.

X.   Liao, L., Zhang, Q., Su, Z., Zhao, Z., Wang, Y., Li, Y., &Cai, X. (2014). Efficient solar water-splitting using a nanocrystallineCoOphotocatalyst. *Nature nanotechnology*, *9*(1), 69.

XI.   Mukerjee, S., &Srinivasan, S. (1993). Enhanced electrocatalysis of oxygen reduction on platinum alloys in proton exchange membrane fuel cells. *Journal of Electroanalytical Chemistry*, *357*(1-2), 201-224.

XII.   Shi, X., Iqbal, N., Kunwar, S. S., Wahab, G., Kasat, H. A., &Kannan, A. M. (2018). PtCo@ NCNTs cathode catalyst using ZIF-67 for proton exchange membrane fuel cell. *International Journal of Hydrogen Energy*, *43*(6), 3520-3526.

XIII.   Shinozaki, K., Zack, J. W., Richards, R. M., Pivovar, B. S., &Kocha, S. S. (2015). Oxygen reduction reaction measurements on platinum electrocatalysts utilizing rotating disk electrode technique I. Impact of impurities, measurement protocols and applied corrections. *Journal of The Electrochemical Society*, *162*(10), F1144-F1158

XIV.   S. Saher, S. Naqash, B. A. Boukamp, B. Li, C. Xia, H. J. M. Bouwmeester, Influence of ionic conductivity of the nano-particulate coating phase on oxygen surface exchange of La0.58Sr0.4Co0.8Fe0.2O3-δ , *J. Mater. Chem. A*, *5 (3),* 2017, 4991-4999

XV.   Song, E., Shi, C., & Anson, F. C. (1998). Comparison of the behavior of several cobalt porphyrins as electrocatalysts for the reduction of O2 at graphite electrodes. *Langmuir*, *14*(15), 4315-4321.

XVI.   Su, B., Hatay, I., Trojánek, A., Samec, Z., Khoury, T., Gros, C. P., &Girault, H. H. (2010). Molecular electrocatalysis for oxygen reduction by cobalt porphyrins adsorbed at liquid/liquid interfaces. *Journal of the American Chemical Society*, *132*(8), 2655-2662.

XVII.   Xia, B. Y., Yan, Y., Li, N., Wu, H. B., Lou, X. W. D., & Wang, X. (2016). A metal–organic framework-derived bifunctional oxygen electrocatalyst. *Nature Energy*, *1*(1), 15006.

XVIII.   Yang, J., Sun, H., Liang, H., Ji, H., Song, L., Gao, C., &Xu, H. (2016). A highly efficient metal- free oxygen reduction electrocatalyst assembled from carbon nanotubes and graphene. *Advanced Materials*, *28*(23), 4606-4613.

XIX.   Zhang, W., Shaikh, A. U., Tsui, E. Y., &Swager, T. M. (2009). Cobalt porphyrin functionalized carbon nanotubes for oxygen reduction. *Chemistry of Materials*, *21*(14), 3234-3241.

XX.   Zhang, X., Chen, Y., Wang, J., &Zhong, Q. (2016). Nitrogen and fluorine dual- doped carbon black as an efficient cathode catalyst for oxygen reduction reaction in neutral medium. *ChemistrySelect*, *1*(4), 696-702.